

Waveform-Diverse Stretch Processing

Dana M. Hemmingsen¹, Patrick M. McCormick¹, Shannon D. Blunt¹, Christopher Allen¹, Anthony Martone², Kelly Sherbondy², David Wikner²

¹Radar Systems Lab (RSL), University of Kansas, Lawrence, KS

²Army Research Laboratory (ARL), Adelphi, MD

Abstract—Stretch processing is widely used as a means to pulse compress the echoes produced by wideband LFM waveforms at a lower sampling bandwidth while still preserving high range resolution. Here the final fast Fourier transform (FFT) stage is replaced by a compensation transform that permits the use of other chirp-like nonlinear FM (NLFM) waveforms without changing the rest of the RF receive chain, thereby facilitating greater diversity in the use of wideband waveforms for legacy radar systems. The efficacy of this approach is experimentally demonstrated using open-air measurements.

Keywords—Stretch Processing, Nonlinear FM, Waveform Diversity

I. INTRODUCTION

Linear frequency modulated (LFM) chirp waveforms have been used in radar applications for over 50 years [1]. Despite the vast array of new waveforms developed since (see [2,3] and references therein), LFM remains the standard for many radar applications because 1) it is easy to generate, particularly at wide bandwidths that enable high range resolution and 2) a receiver mismatch filter is easily accomplished via tapering to suppress sidelobes. A further implementation advantage of LFM is that stretch processing [4,5] in the receiver allows high range resolution to be achieved without sampling at a rate commensurate with the wide bandwidth of the transmitted waveform. While the result is not surprising, it was analytically shown in [6] that stretch processing can only be employed with LFM waveforms, where the point was made that only the mixing of two LFM waveforms can produce a pure tone for subsequent Fourier transform processing after sampling.

It is interesting to note, though, that there are many examples in the literature (e.g. [7-10]) of compensating for distortion to the ideal LFM structure caused by filtering, impedance mismatches, and other hardware variants in the radar transmitter and receiver [9]. Borrowing from this notion of LFM distortion compensation, here we propose the use of nonlinear FM (NLFM) waveforms (e.g. [11-19]) so as to facilitate greater variety in the wideband signals that are feasible for use with stretch processing.

For traditional stretch processing the Fourier transform is effectively a matched filter bank to the collection of scaled sinusoids produced from the mixing of the LFM waveform with the LFM reference, with delay shifts corresponding to frequency shifts. For NLFM waveforms, a compensated Fourier transform is required that likewise matches to the mixer product of the NLFM waveform and LFM reference for different delay shifts, which still correspond to frequency shifts. The only difference is that instead of a collection of sinusoids, this new instantiation involves the superposition of signals that individually possess some small bandwidth.

To ensure the bandwidth of these individual signals is small, thereby preserving the bandwidth-collapsing benefit

provided by the mixer pre-processing stage for subsequent sampling, an NLFM waveform used in this context should still be chirp-like with characteristics that are sufficiently similar to the reference LFM chirp. In other words, both the waveform and reference should be up or down chirping and the aggregate chirp-rate of the NLFM should be similar to that of the reference LFM.

II. STRETCH PROCESSING

It is useful to start with a quick review of stretch processing (see Fig. 1) to provide a baseline for subsequent modifications. Consider the passband representation of an FM waveform defined over $0 \leq t \leq T$ as

$$s(t) = \cos[2\pi f(t)t] \quad (1)$$

for pulsewidth T and $f(t)$ the instantaneous frequency as a function of time. For LFM we can write

$$f(t) = (f_{\text{start}} - f_{\text{end}}) \frac{t}{T}, \quad (2)$$

where f_{start} and f_{end} are the start and end frequencies.

Let $x(t)$ be the scattering from the illuminated range profile. Ignoring nonlinear effects, the reflected signal captured by the radar is therefore represented by the convolution

$$\tilde{y}(t) = s(t) * x(t) + u(t), \quad (3)$$

with $u(t)$ additive noise and $*$ the convolution operation. This signal is mixed with reference signal $s_{\text{ref}}(t)$, which concurrently reduces the bandwidth and down-converts the signal to intermediate frequency f_{IF} where it is bandpass filtered. This IF signal is represented as

$$y_{\text{IF}}(t) = \Phi_{\text{BPF}}\{s_{\text{ref}}(t) \times \tilde{y}(t)\}, \quad (4)$$

for $\Phi_{\text{BPF}}\{\cdot\}$ the bandpass filtering operation. The IF signal is then mixed to baseband and IQ demodulated yielding the complex signal

$$y(t) = y_I(t) + jy_Q(t) = \Phi_{\text{LPF}}\{y_{\text{IF}}(t) \times \exp(-j2\pi f_{\text{IF}}t)\}, \quad (5)$$

where $\Phi_{\text{LPF}}\{\cdot\}$ is a lowpass filtering operation, and $y_I(t)$ and $y_Q(t)$ are the in-phase and quadrature-phase components of the received signal, respectively, that are subsequently sampled.

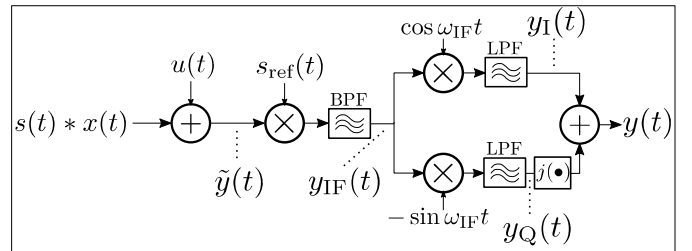


Figure 1. Signal model of stretch processing receive chain

After passing through the RF receive chain in Fig. 1, an LFM waveform reflected from a scatterer at range R would have the complex, baseband response

$$p(t, R) = \Phi_{\text{LPF}} \left\{ \Phi_{\text{BPF}} \left\{ s_{\text{ref}}(t) \times s \left(t - \frac{2R}{c} \right) \right\} \times \exp(-j2\pi f_{\text{IF}} t) \right\} \quad (6)$$

scaled by the amplitude and phase of the particular scatterer, for c the speed of light. For traditional stretch processing, both the transmit signal $s(t)$ and reference signal $s_{\text{ref}}(t)$ are LFM. Therefore, $p(t, R)$ is a sinusoid whose frequency depends on the delay at range R . Thus, in general, $y(t)$ from (5) is a superposition of sinusoids scaled by the amplitudes/phases of the associated range-dependent scattering for which, after sampling, the fast Fourier transform (FFT) serves as a pulse compression matched filter bank.

For the range swath of interest $\Delta R = R_{\text{far}} - R_{\text{near}}$, with R_{near} and R_{far} the near and far range boundaries, the necessary duration of the reference signal is

$$T_{\text{ref}} = T + \Delta\tau, \quad (7)$$

where $\Delta\tau = 2\Delta R / c$ is the delay swath of interest. To capture these ranges, the reference signal $s_{\text{ref}}(t)$ must coincide with time interval $[\tau_{\text{near}}, \tau_{\text{far}} + T]$ for $\tau_{\text{near}} = 2R_{\text{near}} / c$ and $\tau_{\text{far}} = 2R_{\text{far}} / c$, and with $\Delta\tau = \tau_{\text{far}} - \tau_{\text{near}}$. Further, because the IF signal in (4) contains a collection of passband sinusoids that will ultimately become the set of complex baseband sinusoids constituting $y(t)$ in (5), the BPF in (4) must be sufficiently wide to pass the signals corresponding to range interval $[R_{\text{near}}, R_{\text{far}}]$. Thus there is a trade-off between the size of the range interval surveilled and the feasible sampling rate of $y(t)$ without aliasing.

III. WAVEFORM-DIVERSE STRETCH PROCESSING

If the transmitted waveform $s(t)$ deviates from the LFM structure, the mixed product $p(t, R)$ becomes a signal that likewise deviates from a time-windowed sinusoid. Therefore the FFT is no longer the matched filter bank and the bandwidth of the resulting signal is also increased. However, since both $s(t)$ and $s_{\text{ref}}(t)$ are known, the temporal structure of $p(t, R)$ for $R \in [R_{\text{near}}, R_{\text{far}}]$ can be readily determined.

Let T_s be the receiver sampling period for the in-phase and quadrature-phase channels, where $1 / T_s$ must exceed the IF bandwidth for the observed interval of NLFM-LFM mixed products to avoid aliasing. Then, assuming the receive time interval $[\tau_{\text{near}}, \tau_{\text{far}} + T]$ is evenly divisible by T_s , the complex baseband received signal from (5) becomes the length L vector

$$\mathbf{y} = [y(\tau_{\text{near}}) \ y(\tau_{\text{near}} + T_s) \ \dots \ y(\tau_{\text{near}} + (L-1)T_s)]^T \quad (8)$$

for $L = T_{\text{ref}} / T_s$ the sampled duration of the received signal and $(\bullet)^H$ the Hermitian operation.

Sampling $p(t, R)$ in the same manner as (8), we can define the structure of the response from a scatterer at range R for the associated NLFM-LFM mixed product as

$$\mathbf{p}(R) = [p(\tau_{\text{near}}, R) \ \dots \ p(\tau_{\text{near}} + (L-1)T_s, R)]^T, \quad (9)$$

which is likewise length L . Normalizing (9) yields the mixed NLFM-LFM matched filter for range R as

$$\mathbf{w}(R) = \frac{1}{\|\mathbf{p}(R)\|_2} \mathbf{p}(R), \quad (10)$$

and the subsequent matched filter estimate of the scattering at range R as

$$\hat{x}(R) = \mathbf{w}^H(R) \mathbf{y}, \quad (11)$$

for $(\bullet)^H$ the Hermitian operation. The set of mixed NLFM-LFM matched filters can be collected into the $L \times N$ compensation matrix

$$\mathbf{W} = [\mathbf{w}(R_{\text{near}}) \ \mathbf{w}(R_{\text{near}} + \delta R) \ \dots \ \mathbf{w}(R_{\text{near}} + (N-1)\delta R)], \quad (12)$$

where δR is the range sample spacing and $N = \Delta R / \delta R$ is the number of samples in the estimated range profile. This compensation matrix can then be applied to the $L \times 1$ receive data vector to obtain the entire mixed NLFM-LFM matched filter estimate as

$$\hat{\mathbf{x}} = \mathbf{W}^H \mathbf{y}. \quad (13)$$

It is important to note that, since a primary benefit of stretch processing is to obtain high range resolution without sampling at the rate commensurate with a wideband waveform's bandwidth, this waveform-diverse formulation should avoid excessively increasing the IF bandwidth that results from mixing the NLFM waveform and the LFM reference. As such, non-chirped waveforms such as FM implementations of arbitrary polyphase codes [20] or FM noise waveforms [21] are not recommended. However, the "sideways S" time-frequency structure associated with good NLFM waveforms (see [11-19]) does retain a dominant chirp-like characteristic because the prominent delay-Doppler ridge in the ambiguity function is preserved which, according to the "conservation of ambiguity" [3], serves to absorb a significant portion of the fixed amount of ambiguity.

IV. EXPERIMENTAL FORMULATION

This waveform-diverse stretch processing formulation was evaluated in hardware via an open-air experiment. Three different transmit waveforms were implemented: 1) standard LFM to provide a performance baseline, 2) NLFM constructed from piece-wise LFM and compacted to cover the same swept bandwidth as the baseline LFM, and 3) another NLFM constructed using piece-wise LFM, albeit with the same chirp rate as the baseline LFM and higher chirp rates at the edges. For ease of reference, these waveforms are denoted as LFM, NLFM-1, and NLFM-2, respectively (see Fig. 2).

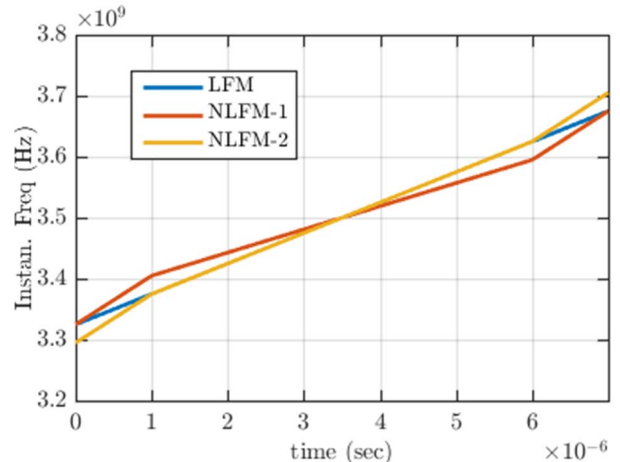


Figure 2. Time-frequency structure of the 3 transmitted waveforms used for testing

Each of the three waveforms was emitted with a center frequency of $f_c = 3.5$ GHz. On receive, the resulting echoes were mixed to the intermediate frequency $f_{IF} = 500$ MHz using an LFM reference signal. The mixed products were then bandpass filtered, down-converted, and IQ sampled using a Rohde & Schwarz real-time spectrum analyzer (RSA).

For IQ sampling, the RSA has a sampling rate of $f_s = 200$ MHz with an analysis bandwidth of 160 MHz (the lowpass filters). As such, the desired range swath ΔR is set to correspond to a receive frequency band of 100 MHz for the LFM mixed products, with the remaining RSA analysis bandwidth used to capture the additional frequency content that arises for the NLFM cases.

The associated range swath of $\Delta R = 300$ m is set to coincide with the range interval between $R_{near} = 900$ m and $R_{far} = 1200$ m. The corresponding delay swath is $\Delta \tau = 2 \mu\text{s}$, with near delay $\tau_{near} = 6 \mu\text{s}$ and far delay $\tau_{far} = 8 \mu\text{s}$. The chirp rate of the LFM waveform and reference signal are thus set by taking the ratio of the receive frequency band to the delay swath as

$$k = \frac{100 \text{ MHz}}{2 \mu\text{s}} = 50 \frac{\text{MHz}}{\mu\text{s}}. \quad (14)$$

The LFM waveform is set to have a bandwidth of 350 MHz (10% bandwidth for $f_c = 3.5$ GHz). The pulsewidth of the waveform can then be calculated as the ratio of the transmit bandwidth to the chirp rate as

$$T = \frac{350 \text{ MHz}}{50 \text{ MHz}/\mu\text{s}} = 7 \mu\text{s}. \quad (15)$$

Thus, according to (7) the reference LFM duration is

$$T_{ref} = 7 \mu\text{s} + 2 \mu\text{s} = 9 \mu\text{s} \quad (16)$$

and coincides with the time interval [6 μs , 15 μs]. Further, to mix the received echoes to the intermediate frequency of $f_{IF} = 500$ MHz, the reference signal must be centered at $f_{C,ref} = 4$ GHz (3.5 GHz + 500 MHz).

The pulsewidths for the two NLFM waveforms are also set to 7 μs , though their swept bandwidths depend on the instantaneous time-frequency structures. Due to the flared edges and same center chirp rate, the NLFM-2 waveform realizes a swept bandwidth of 410 MHz. Likewise, because it is compacted to have the same 350 MHz swept bandwidth as LFM, the NLFM-1 waveform possesses a lower center chirp rate. Further, because the flared edges tend to contribute less to the overall bandwidth due to their faster transition, NLFM-2 possesses roughly the same 3-dB bandwidth as LFM, while NLFM-1 has a narrower 3-dB bandwidth. Thus LFM and NLFM-2 realize essentially the same range resolution while the resolution for NLFM-1 is slightly lower.

The chirp rates of the flared edges for both NLFM waveforms is set to 80 MHz/ μs which, when mixed with the 50 MHz/ μs chirp rate of the LFM reference, produces a signal with a bandwidth of 60 MHz. Therefore, combined with the 100 MHz receive frequency band that realizes the 300 m range swath, the mixed products generated by the NLFM waveforms completely fill the 160 MHz RSA analysis bandwidth. Figure 3 illustrates the mixed frequency responses for all three waveforms for a hypothetical scatterer in the center of the range

swath ($R = 1050$ m), which corresponds to the IF center frequency of 500 MHz. Note that the LFM frequency response in Fig. 3 is also the LFM matched filter response, and thus it yields the highest peak. Since NLFM-2 has the same center chirp rate, it likewise yields a peak, albeit lower than LFM due to the mismatch at the flared edges. In contrast, the NLFM-1 case does not provide a peak at all since the chirp rates do not match the LFM reference.

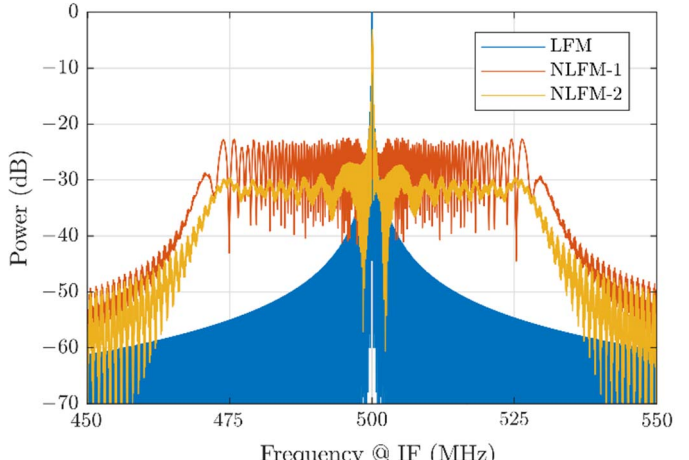


Figure 3. Mixed frequency responses for the three waveforms to a hypothetical scatterer at range 1050 meters. Application of the FFT is standard stretch processing.

If the appropriate compensation transforms for the NLFM-1 and NLFM-2 waveforms from Sec. III are applied to these cases instead of the FFT, then the responses in Fig. 4 are realized. Note that these NLFM waveforms were selected for convenience of demonstration and not for their sidelobe performance, which is slightly better than LFM very close to the mainlobe (see Fig. 4 inset) but with a slower roll-off further out. That said, the important take away from this result is that the combination of chirp-like NLFM waveforms and corresponding compensation transforms can indeed enable the use of stretch processing for a much wider array of prospective waveforms. In the next section this capability is demonstrated experimentally with open-air measurements.

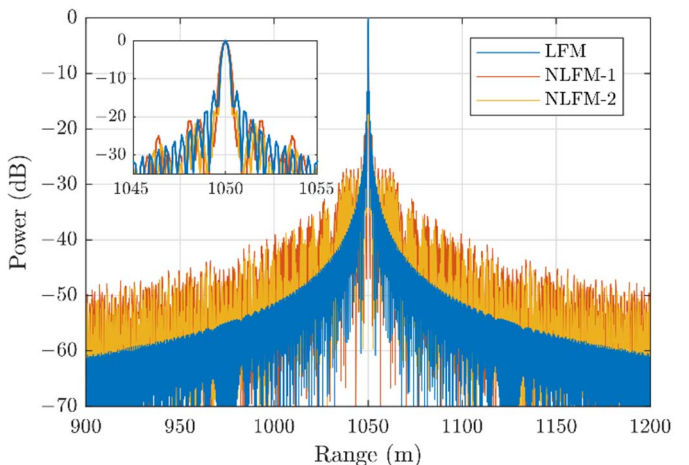


Figure 4. Mixed transform responses (frequency and compensation) for the three waveforms to a hypothetical scatterer at range 1050 meters.

V. OPEN-AIR EXPERIMENTAL RESULTS

The three waveforms, RF receive chain, and associated processing described above are now considered in open-air measurements collected from the rooftop of Nichols Hall on the University of Kansas (KU) campus. For these results, 1000 pulses are coherently combined after stretch processing of each waveform response (with FFT or compensation transform as appropriate). Figures 5 and 6 depict the field of view and hardware instrumentation setup, respectively. Specifically, the field of view includes the 300 m range swath centered on the intersections of 23rd street and Iowa street in Lawrence, KS, which receives a good amount of traffic. Two identical dish antennas with 12.3° beamwidth were used for separate transmit and receive, as shown in Fig. 6.



Figure 5. Field of view for open-air measurements with 12.3° antenna beam



Figure 6. Hardware instrumentation setup for open-air measurements

Let us first examine the zero-Doppler response for each waveform. Figures 7-9 depict the responses to the LFM, NLFM-1, and NLFM-2 waveforms, respectively. In Fig. 7, which is the baseline LFM case, multiple scatterers can be observed, with the dominant scatterer believed to be from the building in the northwest corner of the intersection. Figures 8a and 9a likewise show the result of performing standard FFT-based stretch processing for the NLFM waveforms. In the case

of NLFM-1 (Fig. 8a), the lack of a similar chirp rate means that no scatterers are visible, just like what was observed in Fig. 3. The NLFM-2 case in Fig. 9a does reveal the illuminated scatterers, though there is a loss in SNR of about 2 dB due to the chirp rate mismatch at the flared edges of the waveform.

In contrast, Figs. 8b and 9b reveal the zero-Doppler response to the NLFM waveforms when their compensation transforms are employed. Now all the scatterers are clearly visible because the NLFM-LFM mixed products are actually being matched filtered. The different moving targets in the scene notwithstanding, the results involving compensated stretch processing of NLFM waveforms are qualitatively no different from the standard LFM-based version.

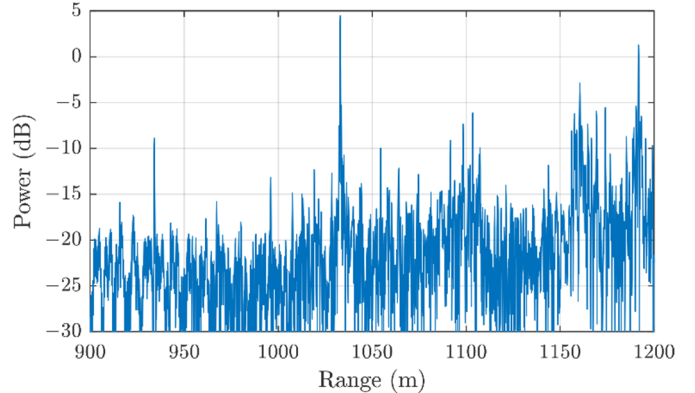


Figure 7. Zero-Doppler range profile for LFM using FFT processing

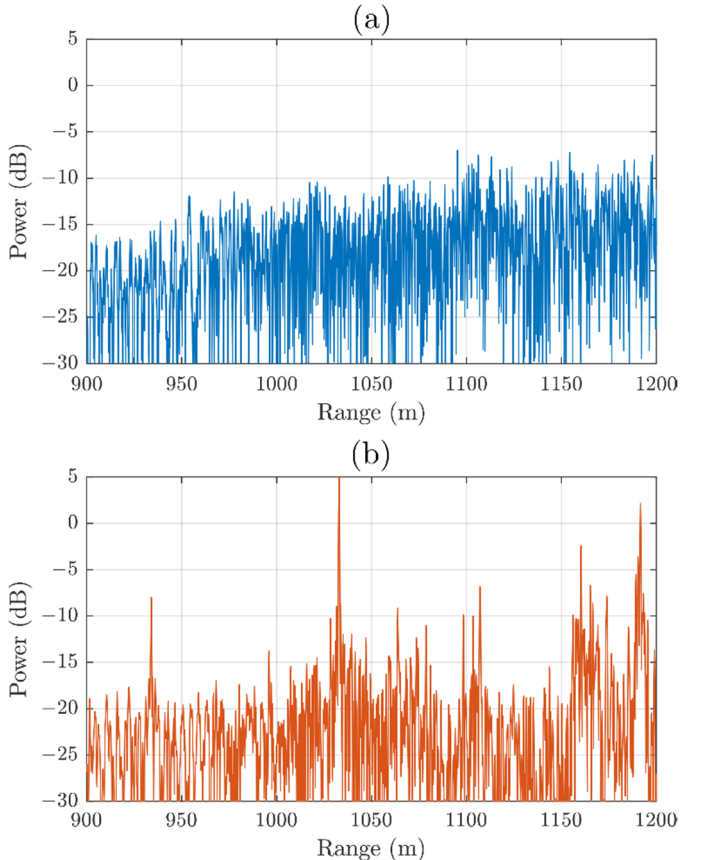


Figure 8. Zero-Doppler range profile for NLFM-1 using (a) FFT processing and (b) the compensation transform

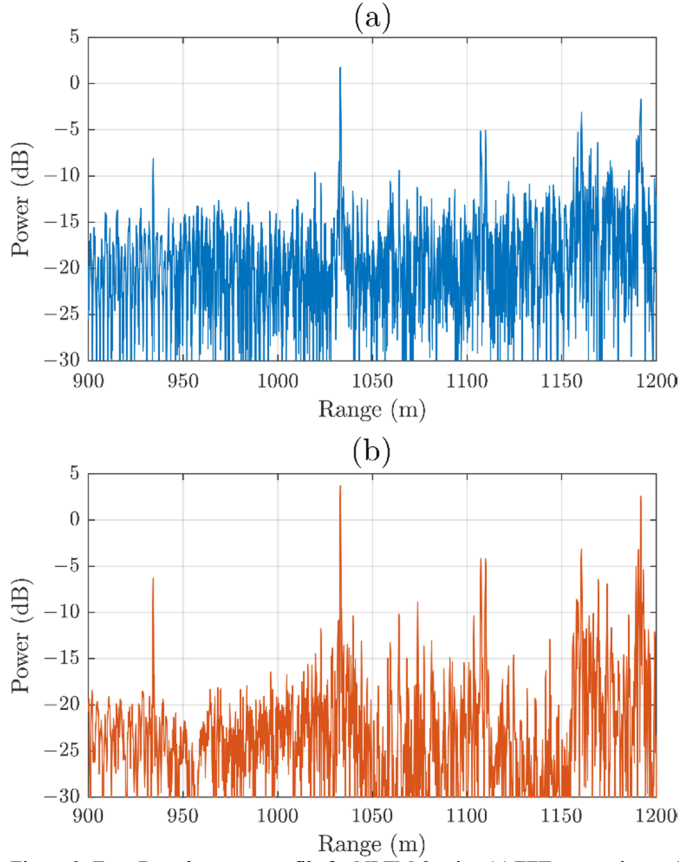


Figure 9. Zero-Doppler range profile for NLFM-2 using (a) FFT processing and (b) the compensation transform

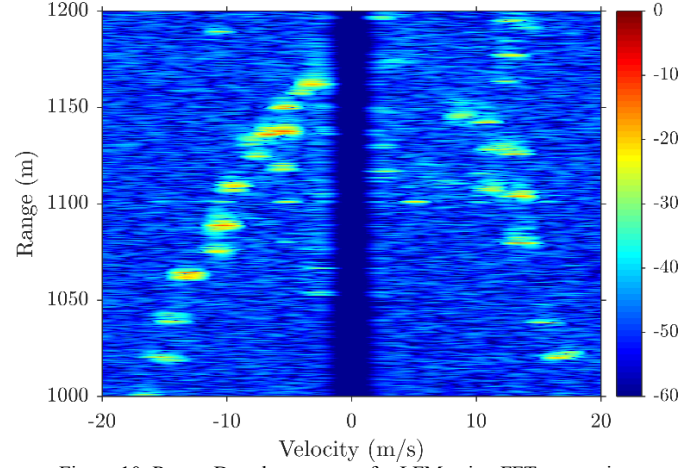


Figure 10. Range-Doppler response for LFM using FFT processing

Now consider Doppler processing and clutter cancellation using these waveforms, noting that the separate waveform CPIs could not capture exactly the same moving target scene. Also, since the instrumentation was stationary, clutter cancellation was performed using a simple zero-Doppler projection. Once again, LFM is used as a baseline and this result is shown in Fig. 10, where multiple vehicles are observed entering/leaving the intersection. Figures 11 and 12 likewise illustrate the problem with attempting to use standard FFT-based stretch processing with the NLFM waveforms, yielding smeared responses

depending upon the degree to which the Fourier transform provides a peak (or not) as observed in Fig. 3. However, the use of the compensation transforms, as depicted in Figs. 13 and 14, addresses the mismatch effect of FFT-processing and reveals the collections of moving targets in the scene, again demonstrating the potential for the use of a much wider array of waveforms for wideband radar applications.

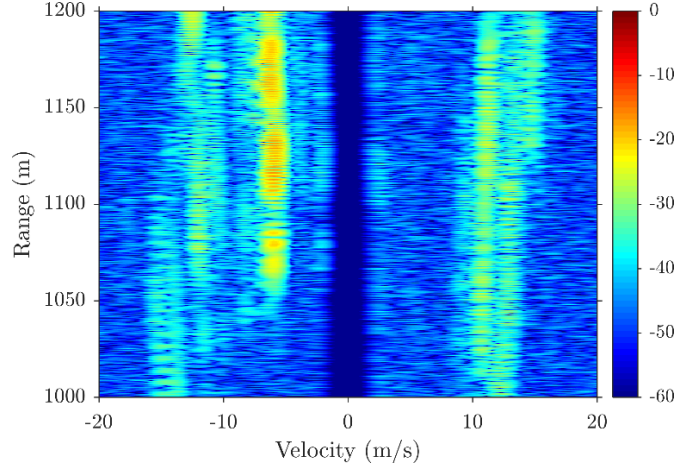


Figure 11. Range-Doppler response for NLFM-1 using FFT processing

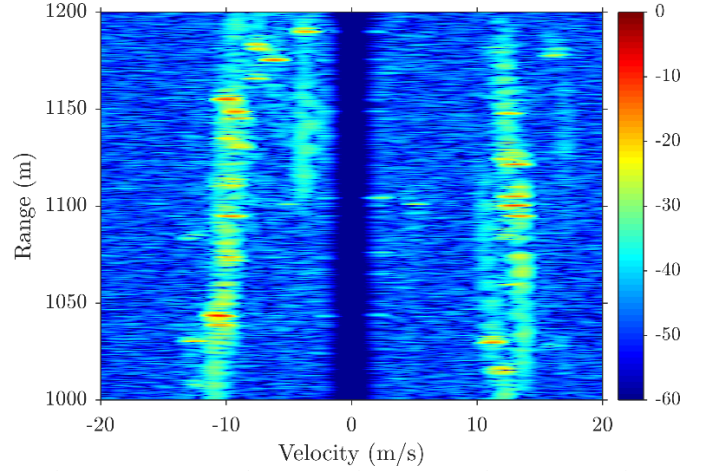


Figure 12. Range-Doppler response for NLFM-2 using FFT processing

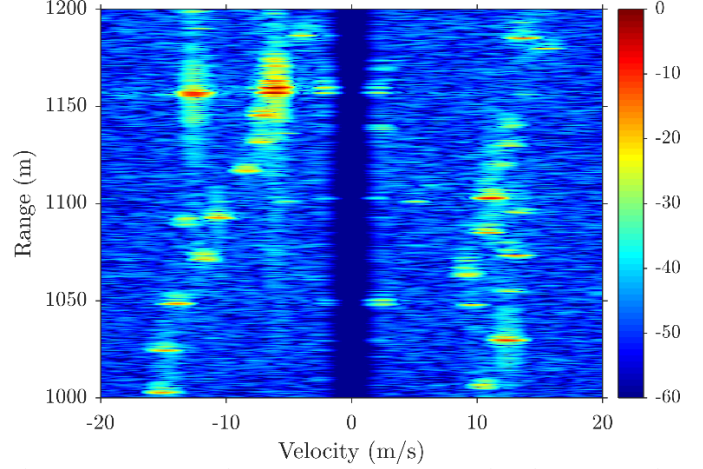


Figure 13. Range-Doppler response for NLFM-1 using the compensation transform (same data as Fig. 11)

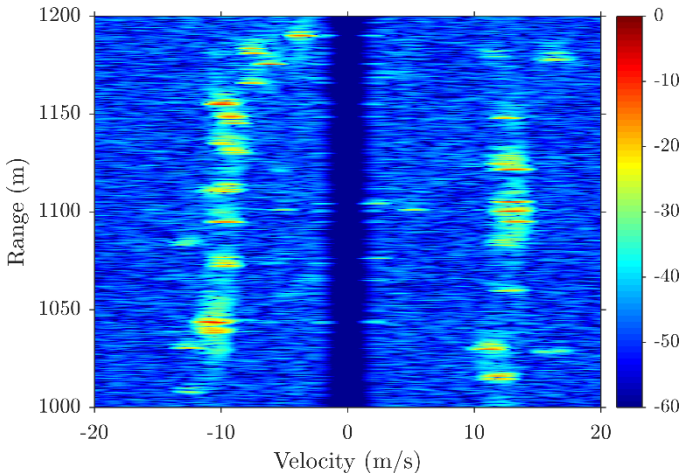


Figure 14. Range-Doppler response for NLFM-2 using the compensation transform (same data as Fig. 12)

VI. CONCLUSIONS

It has been experimentally demonstrated that chirp-like nonlinear FM (NLFM) waveforms can be used with stretch processing as long as an appropriate compensation transform is used in place of the standard FFT. It is interesting to note that, like the DFT from which the FFT emerges, these compensation matrices are matched filter banks to the NLFM-LFM mixer products and likewise possess a frequency-shifted structure across the columns by virtue of LFM reference mixing. It remains to be seen how well optimized NLFM waveforms retain their low sidelobe structure through this process or whether new waveforms need to be designed specifically for this manner of receive processing.

Further, the generalization to chirp-like NLFM waveforms is also applicable for the use of optimal and adaptive mismatch filtering within this stretch processing context as well [22]. The combination of these new waveform and filtering prospects opens up new avenues of research for wideband waveform diversity that are applicable to legacy radar systems that rely on stretch processing.

REFERENCES

- [1] J.R. Klauder, A.C. Price, S. Darlington, W.J. Albersheim, "The theory and design of chirp radars," *The Bell System Technical Journal*, vol. XXXIX, no. 4, pp. 745-808, July 1960.
- [2] N. Levanon and E. Mozeson, *Radar Signals*, Wiley-IEEE Press, 2004.
- [3] S.D. Blunt, E.L. Mokole, "An overview of radar waveform diversity," *IEEE AESS Systems Magazine*, vol. 31, no. 11, pp. 2-42, Nov. 2016.
- [4] W.J. Caputi, "Stretch: a time-transformation technique," *IEEE Trans. Aerospace & Electronic Systems*, vol. AES-7, no. 2, pp. 269-278, Mar. 1971.
- [5] W.L. Melvin, J.A. Scheer, eds., *Principles of Modern Radar, Vol. II: Advanced Techniques*, SciTech Publishing, Edison, NJ, 2013, p. 26-40.
- [6] L. Yeh, K.T. Wong, H.S. Mir, "Viable/inviable polynomial-phase modulations for 'stretch processing,'" *IEEE Trans. Aerospace & Electronic Systems*, vol. 48, no. 1, pp. 923-926, Jan. 2012.
- [7] H.D. Griffiths, "The effect of phase and amplitude errors in FM radar," *IEE Colloquium on High Time-Bandwidth Product Waveforms in Radar & Sonar*, May 1991.
- [8] D.J. Rabideau, "Adaptive waveform distortion compensation," *39th Asilomar Conf. on Signals, Systems, & Computers*, Pacific Grove, CA, Oct./Nov. 2005.
- [9] H. Krichene, E. Brawley, K. Lauritzen, A. Wu, S. Talisa, "Time sidelobe correction of hardware errors in stretch processing," *IEEE Trans. Aerospace & Electronic Systems*, vol. 48, no. 1, pp. 637-647, Jan. 2012.
- [10] Y.-X. Zhang, R.-J. Hong, P.-P. Pan, Z.-M. Deng, Q.-F. Liu, "Frequency domain range sidelobe correction in stretch processing for wideband LFM radars," *IEEE Trans. Aerospace & Electronic Systems*, vol. 53, no. 1, pp. 111-121, Feb. 2017.
- [11] C.E. Cook, "A class of nonlinear FM pulse compression signals," *Proc. IEEE*, vol. 52, no. 11, pp. 1369-1371, Nov. 1964.
- [12] E. Fowle, "The design of FM pulse compression signals," *IEEE Trans. Information Theory*, vol. 10, no. 1, pp. 61-67, Jan. 1964.
- [13] I. Gladkova, "Design of frequency modulated waveforms via the Zak transform," *IEEE Trans. Aerospace & Electronic Systems*, vol. 40, no. 1, pp. 355-359, Jan. 2004.
- [14] A.W. Doerry, "Generating nonlinear FM chirp waveforms for radar," *Sandia Report*, SAND2006-5856, Sept. 2006.
- [15] S.D. Blunt, J. Jakabosky, M. Cook, J. Stiles, S. Seguin, and E.L. Mokole, "Polyphase-coded FM (PCFM) radar waveforms, part II: optimization," *IEEE Trans. Aerospace & Electronic Systems*, vol. 50, no. 3, pp. 2230-2241, July 2014.
- [16] J. Jakabosky, S.D. Blunt, and B. Himed, "Optimization of 'over-coded' radar waveforms," *IEEE Radar Conf.*, Cincinnati, OH, May 2014.
- [17] P.S. Tan, J. Jakabosky, J.M. Stiles, and S.D. Blunt, "On higher-order representations of polyphase-coded FM radar waveforms," *IEEE Intl. Radar Conf.*, Arlington, VA, May 2015.
- [18] P.M. McCormick and S.D. Blunt, "Nonlinear conjugate gradient optimization of polyphase-coded FM radar waveforms," *IEEE Radar Conference*, Seattle, WA, May 2017.
- [19] P.M. McCormick and S.D. Blunt, "Gradient-based coded-FM waveform design using Legendre polynomials," *IET International Conference on Radar Systems*, Belfast, UK, Oct. 2017.
- [20] S.D. Blunt, M. Cook, J. Jakabosky, J. de Graaf, E. Perrins, "Polyphase-coded FM (PCFM) radar waveforms, part I: implementation," *IEEE Trans. Aerospace & Electronic Systems*, vol. 50, no. 3, pp. 2218-2229, July 2014.
- [21] J. Jakabosky, S.D. Blunt, B. Himed, "Spectral-shape optimized FM noise radar for pulse agility," *IEEE Radar Conf.*, Philadelphia, PA, May 2016.
- [22] L. Harnett, D. Hemmingsen, P. McCormick, S.D. Blunt, C. Allen, A. Martone, K. Sherbondy, D. Wikner, "Optimal and adaptive mismatch filtering for stretch processing," *IEEE Radar Conf.*, Oklahoma City, OK, Apr. 2018.